Nonlinear effects in charge stabilized colloidal suspensions

T. Kreer, J. Horbach,* and A. Chatterji

Institut für Physik, Johannes-Gutenberg-Universität, 55099 Mainz, Germany

(Received 18 January 2006; published 3 August 2006)

Molecular-dynamics simulations are used to study the effective interactions in charged stabilized colloidal suspensions. We focus on highly charged macroions in the limit of low salt concentrations. Within this regime, nonlinear corrections to Debye-Hückel (DH) theory have to be considered. For non-bulk-like systems, such as isolated pairs or triples of macroions, we show that nonlinear effects can become relevant, which cannot be described by the charge renormalization concept [S. Alexander *et al.*, J. Chem. Phys. **80**, 5776 (1984)]. For an isolated pair of macroions, we find an almost perfect qualitative agreement between our simulation data and DH theory. However, on a quantitative level, neither DH theory nor the charge renormalization concept can be confirmed in detail. This seems mainly to be related to the fact that for small ion concentrations, microionic layers can strongly overlap, whereas, simultaneously, excluded volume effects are less important. In the case of isolated triples, where we compare between coaxial and triangular geometries, we find attractive corrections to pairwise additivity in the limit of small macroion separations and salt concentrations. These triplet interactions arise if all three microionic layers around the macroions exhibit a significant overlap. In contrast to the case of two isolated colloids, the charge distribution around a macroion in a triple is found to be anisotropic.

PACS number(s): 82.70.Dd, 61.20.Ja

I. INTRODUCTION

[1]In order to simplify the description of colloidal systems, one often tries to determine effective interactions between the colloidal particles, thus integrating out the solvent's degrees of freedom [1]. This is not a trivial task, because in general the effective interactions depend on the thermodynamic state of the system, and one is often confronted with the problem of thermodynamic inconsistencies [2]. A problem that is of particular interest is that of effective interactions between charged colloids (macroions) in an electrolyte solution. On a mean-field level, such a system can be described by the Poisson-Boltzmann (PB) equation [3]. The linearized version of this equation is the basis of the Derjaguin-Landau-Verwey-Overbeek (DLVO) theory for charged colloids [4], and we will refer to it in the following as the Debye-Hückel (DH) limit of the PB equation [5]. In the DH limit, the problem can be solved analytically and yields a screened Coulomb potential for the effective interactions between the macroions. The characteristic range of this potential is given by the Debye length κ^{-1}, which is controled by solvent properties such as the salt concentration.

The physical picture of the DH description is rather appealing: Due to the charge of a macroion, a layer of thickness κ^{-1} is formed around it, consisting of oppositely charged microions (counterions), leading to a screening of the bare Coulomb interaction. Although the DH description is only valid for weakly charged macroions and if correlation effects between the microions in the electrolyte solution can be neglected, it is tempting to characterize also the effective interactions between highly charged macroions by a potential of screened Coulomb form. Indeed, this is the idea of the famous concept of charge renormalization that has been put

forward by Alexander *et al.* [6]. It is based on the observation that in the framework of the so-called cell model (see below), the numerical solution of the nonlinear PB equation can be fitted farther away from the macroions' boundaries by a screened Coulomb potential with a renormalized charge $Z_{\text{eff}} < Z$ (with Z the bare charge of a macroion). Trizac *et al.* [7] recently extended the numerical recipe of Alexander *et al.* by providing an analytical scheme to calculate Z_{eff} as well as the effective screening length and the effective salt concentration.

As already mentioned, DH theory is based on the linearized PB equation, which implies pairwise additivity of interaction energies (on the level of the macroions). On the other hand, for highly charged macroions, nonlinearities imply the occurrence of many-body interactions and thus pairwise additivity does not hold. The simplest system, in which many-body effects could be expected, consists of three isolated macroions in an electrolyte solution. Indeed, such a system has been studied in a recent experiment using scanned optical line tweezers [8,9]. In this work, charge stabilized silica particles with a diameter of about 1 μm suspended in water were considered. It was possible to measure three-body interactions directly, and it was found that, in agreement with numerical solutions of the nonlinear PB equation [1,10], three-body contributions to the total interaction energy are attractive.

Also molecular-dynamics (MD) computer simulations have been used to investigate systems of "isolated" macroion pairs and triples [11–15]. In these studies, charged colloids were investigated in the framework of the so-called primitive model. In this model, a system of macroions, counterions, and salt ions is considered without explicitly taking into account the uncharged part of the solvent. Based on the primitive model, Allahyarov and Löwen found that DH theory works well for a system of two macroions [11], and, in agreement with experiment [8,9] and PB theory [16], that three-body contributions are attractive in the case of three macroions [12]. These authors also studied a system of two

---

*Electronic address: horbach@uni-mainz.de

macroions, in which uncharged solvent particles were added to the electrolyte solution [13]. An interesting finding of this work was that the neutral solvent leads to a renormalized charge, which is smaller than the bare charge of the macroions, similar to the concept proposed by Alexander *et al.* [6]. In a different simulation study by Tehver *et al.* [14], the counterions were introduced via density distributions in the framework of a density-functional theory. Surprisingly, in the case of three macroions, no evidence for many-body forces was found, and the forces could be well described by DH theory.

In this work, MD simulations are presented that tie in with the previous simulation studies. However, we extend the latter studies by investigating systematically the effect of salt concentration on colloidal interactions in systems of two and three isolated macroions. Compared to previous studies, this allows a more detailed discussion of nonlinear effects in such systems and a quantitative test of pairwise additivity in the case of three macroions.

We consider systems of two and three highly charged macroions in a primitive model solvent. In the two-particle case, we check to what extent DH theory describes the effective interactions; thereby, the effect of nonlinearities is quantified. In a second step, we address the influence of nonlinear effects on three-body interactions. In order to study these effects, a triple of macroions is considered in two different geometries by placing the macroions on an equilateral triangle or along a straight line. We check whether the concept of charge renormalization can also be applied to isolated pairs or triples of particles. Furthermore, we ask for the validity of the mean-field description and how effective interactions develop from the two-particle case to the bulk. Our major concern is the influence of nonlinearity, which can be seen for high macroion charges and low salt concentrations. We especially consider cases of overlapping or interacting Debye layers in the case of non-bulk-like macroion configurations.

Our paper is organized as follows: After briefly discussing some results of DH theory and the concept of charge renormalization, we give an overview of the simulation details. In Sec. IV A, we present our results for systems that consist of a pair of macroions, and in Sec. IV B, systems with macroion triples are considered. Finally, we discuss the results and draw some conclusions.

II. DH POTENTIAL, PB EQUATION, AND THE CONCEPT OF CHARGE RENORMALIZATION

In this section, we consider charged spherical macroions of diameter σ and positive charge Ze (here, e is the elementary charge and Z is the valency). They are immersed into a polar, structureless medium with dielectric constant ϵ. This medium is characterized by the Bjerrum length $\lambda_B = e^2/(4\pi\epsilon k_B T)$, i.e., the distance at which the electrostatic energy between two point charges equals the thermal energy $k_B T$.

In the DH limit, the interaction potential between two macroions, separated by a distance r, is given by a screened Coulomb (Yukawa) potential [3],

$$u(r) = k_B T \lambda_B \left[\frac{Z \exp(\kappa\sigma/2)}{1 + \kappa\sigma/2} \right]^2 \frac{\exp(-\kappa r)}{r}, \tag{1}$$

where

$$\kappa = \sqrt{4\pi\lambda_B(2n_s + Zn_c)/V} \tag{2}$$

is the screening parameter, n_c represents the number of macroions, and n_s is the number of added salt ion pairs. In Eq. (2), it is assumed that the electrolyte solution is formed by monovalent microions in a system of total volume V. The microions consist of Zn_c negatively charged counterions that neutralize the charge of the macroions and $2n_s$ salt ions, consisting of half counterions and half oppositely charged coions. The inverse of the screening parameter, the so-called Debye length $R_D = 1/\kappa$, "measures" the thickness of the neutralizing counterion layer around the macroions. Equation (2) shows that R_D can be varied by changing the properties of the solvent, in particular the salt concentration.

Alexander *et al.* [6] have demonstrated that many charged colloidal systems with highly charged macroions can be described to some extent by a Yukawa potential of the form of Eq. (1), although the DH limit is restricted to particles with small charge.

Highly charged colloids have a strong tendency to form ordered structures at relatively low densities, i.e., at densities where the mean distance between neighboring macroions is much larger than their size. In such systems, each macroion has a very similar environment of microions, and thus a reasonable approximation is to reduce the problem of computing the effective many-particle interactions between macroions to that of determining a mean-field potential of one particle in its Wigner-Seitz (WS) cell surrounded by a reservoir of salt ions [6]. For spherical macroions, the WS cell is approximated by a sphere of radius R. Then, one considers the nonlinear PB equation for the single particle with appropriate boundary conditions [6],

$$\nabla^2 u(r) = \frac{e\rho_s}{4\pi\epsilon} \left[\exp\left(\frac{eu(r)}{k_B T}\right) - \exp\left(-\frac{eu(r)}{k_B T}\right) \right]$$

$$(\sigma/2 < r < R), \tag{3}$$

$$\vec{n} \cdot \nabla u(r) = \frac{Ze}{\pi\epsilon\sigma^2} \quad (r = \sigma/2), \tag{4}$$

$$\vec{n} \cdot \nabla u(r) = 0 \quad (r = R) \tag{5}$$

with $\vec{n}$ the normal vector pointing outward from the sphere's surface and ρ_s the salt concentration in the reservoir. From Eq. (3) with boundary conditions (4) and (5), an effective charge Z_{eff} and an effective screening parameter κ_{eff} can be extracted that can be used to define an effective Yukawa potential,

$$u_{\text{eff}}(r) = k_B T \lambda_B \left[\frac{Z_{\text{eff}} \exp(\kappa_{\text{eff}}\sigma/2)}{1 + \kappa_{\text{eff}}\sigma/2} \right]^2 \frac{\exp(-\kappa_{\text{eff}} r)}{r}. \tag{6}$$

In the original paper by Alexander *et al.* [6], the following recipe has been proposed to obtain Z_{eff} and κ_{eff}: The screening parameter κ_{eff} is determined by the microion den-

sities $n_\pm^R = \rho_0 \exp[\pm eu(r)/(k_B T)]$ at the WS cell boundary via $\kappa_{\mathrm{eff}}^2 = 4\pi\lambda_B(n_+^R + n_-^R)$. The effective charge Z_{eff} is fixed as follows: First, Eq. (3) is linearized at $r=R$. For the linearized equation, a solution is determined such that the linear and the nonlinear solution match up to the second derivative at the cell boundary. Finally, Z_{eff} is calculated from the integral over the charge density associated with the linear solution.

A more elegant recipe to obtain Z_{eff} and κ_{eff} has recently been proposed by Trizac et al. [7]. They show that the full numerical solution of the nonlinear PB equation is not needed to estimate the latter parameters. Instead, only the solution u_R at the cell boundary is required. Thus, only linearized equations have to be solved, and this can be done analytically. For Z_{eff}, Trizac et al. [7] find

$$Z_{\mathrm{eff}} = \frac{\gamma_0}{\kappa_{\mathrm{eff}}\lambda_B}\{(\kappa_{\mathrm{eff}}^2\sigma R/2 - 1)\sinh[\kappa_{\mathrm{eff}}(R - \sigma/2)] + \kappa_{\mathrm{eff}}(R - \sigma/2)\cosh[\kappa_{\mathrm{eff}}(R - \sigma/2)]\}, \quad (7)$$

with $\gamma_0 = \tanh(u_R)$. Equation (7) implies $Z_{\mathrm{eff}} \lesssim Z$, where the effective charge (also called "renormalized charge") can be an order of magnitude smaller than the bare charge.

The effective screening parameter κ_{eff} is related to the effective salt concentration and Z_{eff} via [7]

$$n_s^{\mathrm{eff}}/V = \frac{\kappa_{\mathrm{eff}}^2}{8\pi\lambda_B}(1 - \gamma_0^2)(1 - \eta) - \frac{1}{2V}Z_{\mathrm{eff}}n_c(1 - \gamma_0), \quad (8)$$

where n_s^{eff}/V is the salt concentration (with V the volume of the system) and $n_c=1$ represents the number of macroions per WS cell. The physical interpretation of the latter equation is related to the so-called Donnan effect. Since a macroion occupies a finite volume inside its WS cell, the microions are partially expelled. Thus, the salt concentration outside the WS cell can be higher than inside the colloid compartement, or, in other words, there is an effective salt concentration that is smaller than the actual one, i.e., $n_s^{\mathrm{eff}} < n_s$.

For dilute systems, where the Donnan effect should not be relevant, i.e., for $\gamma_0, \eta \to 0$, the effective salt concentration matches the actual one, and hence Eq. (8) can be rewritten as

$$\kappa_{\mathrm{eff}}^2 = 4\pi\lambda_B(Z_{\mathrm{eff}}n_c + 2n_s)/V. \quad (9)$$

Thus, setting $n_s^{\mathrm{eff}} = n_s$ leads back to a one-parameter problem. It follows from Eq. (9) that for monovalent microions, $Z_{\mathrm{eff}} = Z$ also implies $\kappa_{\mathrm{eff}} = \kappa$.

We emphasize that the systems considered in the following do not match with the assumptions made in Alexander's concept of charge renormalization. In this work, "non-bulk-like" systems are considered, for which the definition of a WS cell is not meaningful. Moreover, whereas charge renormalization is applied to distances far away from the surface of a macroion, we are interested in relatively small distances between macroions and thus also in the potential of mean force close to their surfaces.

III. DETAILS OF THE SIMULATION

Using classical MD simulations, we study charged colloidal suspensions in the framework of the so-called primitive model. We consider systems of two or three positively charged macroions of valency $Z \equiv Z_m = 255$ and monovalent microions of valency $Z_{\mathrm{ct}} = -1$ (counterions) and of valency $Z_{\mathrm{co}} = +1$ (coions). The interaction potential between an ion of type α and an ion of type β ($\alpha, \beta = m, \mathrm{ct}, \mathrm{co}$), separated by a distance r from each other, is given by

$$u_{\alpha\beta} = \frac{Z_\alpha Z_\beta e^2}{4\pi\epsilon r} + A_{\alpha\beta}\exp\{-B_{\alpha\beta}(r - \sigma_{\alpha\beta})/\sigma_{\alpha\beta}\}, \quad (10)$$

where the dielectric constant is set to $\epsilon = 79\epsilon_0$ (with ϵ_0 the vacuum dielectric constant), which corresponds to the value for water at room temperature. The parameter $\sigma_{\alpha\beta}$ is the distance between two ions at contact, $\sigma_{\alpha\beta} = R_\alpha + R_\beta$, where R_α is the radius of an ion of type α. In our simulations, we used $R_m = 10$ nm and $R_{\mathrm{ct}} = R_{\mathrm{co}} = 0.01R_m$. The choice of the latter values guarantees that depletion effects are not relevant. The exponential in Eq. (10) is an approximation to a hard-sphere interaction for two ions at contact. For the parameters $A_{\alpha\beta}$ we chose $A_{mm} = 1.84$ eV, $A_{mct} = A_{mco} = 0.055\,65\,44$ eV, and $A_{ctct} = A_{ctco} = A_{coco} = 0.0051$ eV. The parameters $B_{\alpha\beta}$ are all set to 3.0. The long-ranged Coulomb part of the potential and the forces were computed by Ewald sums in which we chose $\alpha = 0.05$ for the constant and a cutoff wave number $k_c = 2\pi\sqrt{66}/L$ in the Fourier part [17]. The linear dimension L of the simulation box is $L = 159.026$ nm, using periodic boundary conditions.

Since the potential, Eq. (10), is long-ranged, one has to consider the possible emergence of finite-size effects. However, in our simulations, the distance of a macroion to its next periodic image was always larger than 7σ (with $\sigma \equiv \sigma_{mm}$), and, as discussed in the next section, at this distance the Coulomb interaction is sufficiently screened. Instead of using periodic boundary conditions, an alternative approach would be to confine the system by walls [11,12]. However, due to the interaction of the ions with the walls, also in this case finite-size effects are relevant (indeed in Refs. [11,12], a correction term had to be introduced to estimate the "bulk" effective force between macroions).

In order to determine the effective forces between macroions at a distance r, the macroions are fixed by decoupling macroionic and microionic time scales. This is achieved by assigning a mass to the macroion which is $10^6 m_{\mathrm{ct}}$ (with $m_{\mathrm{ct}} = m_{\mathrm{co}}$ the mass of the microions). All the simulations were done at the temperature $T = 298$ K. Thus, the Bjerrum length for our system is $\lambda_B \approx 0.71$ nm. The number of added coions was varied from $n_s = 0$ to $n_s = 1280$. In molar units, this corresponds to an added salt concentration from 0 to 1.06×10^{-3} mol/l. Being n_c' the number of macroions in the system, charge neutrality requires $n_{\mathrm{tot}} = Zn_c' + 2n_s$ for the total number of microions.

The equations of motion were integrated using the velocity form of the Verlet algorithm. The simulations were done at constant temperature. In order to thermostat the system, it was coupled to a stochastic heat bath [17]. For a given set of parameters (n_s, macroion separation r), we examined at least three independent start configurations. For equilibration, runs of $10^5 - 10^6$ MD time steps were done, followed by a similar number of steps to calculate time averages. Depending on
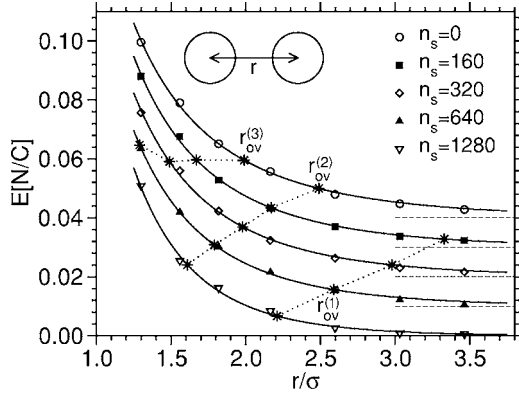
FIG. 1. Electric field around macroion as a function of distance for indicated salt concentrations. Solid lines are fits to Eq. (6), where Z_{eff} and κ_{eff} are used as fit parameters. Data are shifted such that the dotted lines represent an electric field of $E=0$ for each value of n_s. Stars indicate critical macroion separations, as defined in the text. Dashed lines are guides to the eye. Statistical errors are smaller than twice the size of the symbols. In molar units, the concentration of added salt varies from 0 to 1.06×10^{-3} mol/l.

salt concentration, the time step varied from $\Delta t = 1 \times 10^{-4} \tau_0$ to $\Delta t = 3 \times 10^{-4} \tau_0$ [with $\tau_0 \equiv R_{ct} \sqrt{m_{ct}/(k_B T)}$].

IV. RESULTS AND DISCUSSION

A. Two macroions

The effective interaction between two macroions can be measured by the quantity $E(r) \equiv \frac{1}{Ze} F(r)$, depending on the separation r between the macroion's centers. Here, $F(r) = -\partial V(r)/\partial r$ is the total force on a macroion projected onto the line that connects the macroion's centers. Figure 1 shows $E(r)$ for different salt concentrations, as indicated. A comparison to the prediction from DH theory, using $u_{eff}(r)$ from Eq. (6), with Z_{eff} and κ_{eff} as fitting parameters, reveals a good agreement. However, as we will show in the following, the numerical values we obtain for Z_{eff} and κ_{eff} can be described neither by the DH predictions nor by the charge renormalization concept, as it results in Eqs. (7) and (8). Plotting our data on a logarithmic scale exposes deviations from the DH form (Fig. 2), which seem to increase with distance and salt concentration. We confirmed the absence of finite-size effects by repeating some of our simulation runs in a system of double volume, finding our results to be consistent and not depending on the volume.

To analyze our data further, it is useful to quantify the extent to which the Debye layers around the macroions overlap. To this end, we use the DH expression, Eq. (2), to estimate the inverse Debye layer thickness. According to this definition of κ, Debye layers overlap, if $\frac{\kappa \sigma}{2}(\frac{r}{\sigma}-1) < 1$. For a given value of n_s we thus define $r_{ov}^{(1)} \equiv \sigma + 2\kappa^{-1}$ as the smallest macroion separation where their Debye layers do not overlap. For $\kappa \sigma (\frac{r}{\sigma}-1) < 1$, the macroions are (partially) located within each other's Debye layers. For a fixed salt concentration, we therefore define $r_{ov}^{(2)} \equiv \sigma + \kappa^{-1}$. Finally, we consider the limit where a macroion's center of mass is located
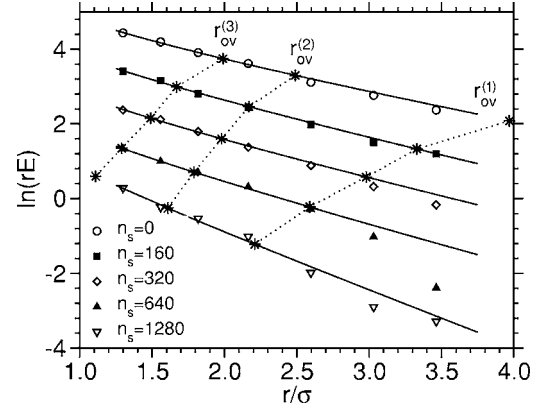

FIG. 2. Logarithm of electric field times macroion separation vs r for various salt concentrations. Solid lines are fits to Eq. (6) using the same fitting parameters as in Fig. 1. Data for $n_s=0$ are shifted by 4, $n_s=160$ by 3, $n_s=320$ by 2, and $n_s=640$ by 1, respectively. Stars and dashed lines have same meaning as in Fig. 1.

within the Debye layer of the other macroion. This is the case for $\kappa \sigma (\frac{r}{\sigma}-\frac{1}{2}) < 1$, or $r_{ov}^{(3)} \equiv \sigma/2 + \kappa^{-1}$. The radii $r_{ov}^{(1,2,3)}$ are indicated in Figs. 1 and 2 as stars (connected by dashed lines as a guide to the eye).

As we see in Figs. 1 and 2, Debye layers overlap for almost all parameter combinations considered. Thus, we find a Yukawa-like potential also in the region of strongly overlapping Debye layers. The Yukawa form persists even for macroion separations $r < r_{ov}^{(3)}$, where the macroions are relatively close to contact. These findings are in agreement with numerical solutions of the nonlinear PB equation for a system of two macroions [16]. The significant deviations from the DH fits seem to occur for nonoverlapping Debye layers (see Fig. 2). This might be related to the low signal-to-noise ratio, which becomes worse for increasing values of κr. Note that the fits in Fig. 2 use the derivative of Eq. (6) as a fit formula for E (multiplied by $-1/Ze$, of course). In a plot of $\ln(rE)$ versus r, this implies the occurrence of a nonlinear logarithmic term. A closer inspection of the solid lines in Fig. 2 shows indeed that the DH fits are not perfect straight lines in the considered range of macroion separations.

Figure 3 shows the fitted values of Z_{eff} and κ_{eff} as a function of salt ion pairs n_s. Here, we have normalized Z_{eff} by the
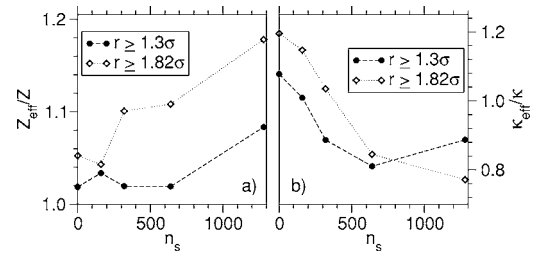

FIG. 3. (a) Effective charge Z_{eff} normalized by the bare charge Z and (b) effective screening parameter κ_{eff} divided by κ from DH theory [Eq. (2)] as a function of the number of salt ion pairs n_s. The parameters Z_{eff} and κ_{eff} result from fits shown in Fig. 1 and Fig. 2 that include, as indicated, all data points with $r \geq 1.3\sigma$ or only those with $r \geq 1.82\sigma$.
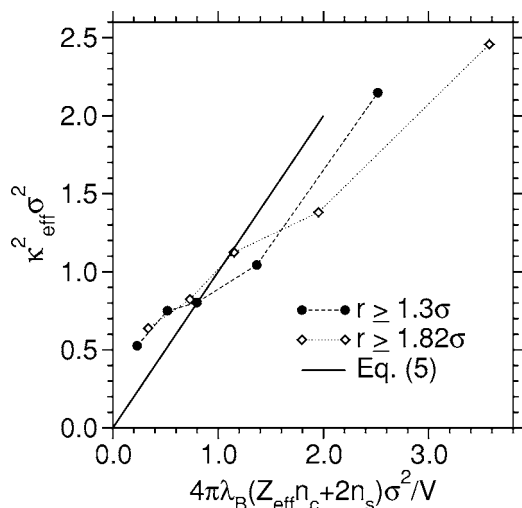
FIG. 4. Test of Eq. (9) in the limit $\eta, \gamma_0 \to 0$.

bare charge of the macroions and κ_{eff} by the screening parameter κ as predicted by Eq. (2). The fit values in Fig. 3 are extracted from two different types of fits. In addition to fits that include all available data points, we performed also fits that are restricted to data points with macroion separations of $r \geq 1.82\sigma > r_{\mathrm{ov}}^{(3)}$. Thus, in the latter fits, we exclude distances for which the center of a macroion penetrates into the Debye layer of the other one.

As one can infer from Fig. 3, $\kappa_{\mathrm{eff}}/\kappa$ and Z_{eff}/Z deviate significantly from unity for all salt concentrations considered (except for $n_s \approx 250$, where $\kappa_{\mathrm{eff}}/\kappa$ is close to 1). Thus, for the systems under consideration, DH theory does not correctly describe the effective interactions. This indicates that a combination of nonlinear effects and, possibly, microionic correlations is relevant in the present case.

Of particular interest is the behavior of Z_{eff}. For all salt concentrations it is larger than the bare charge and it tends to increase with increasing salt content. This effect is even more pronounced if the fits are restricted to macroion separations of $r \geq 1.82\sigma$. This finding is in disagreement with the concept of charge renormalization, where one expects a decrease of the effective charge with increasing salt concentration. Indeed, cell model calculations using the parameters of our MD simulations lead to $Z_{\mathrm{eff}} \approx 0.8Z$ [15].

A failure of the charge renormalization concept in the systems considered here is not surprising. For an isolated pair of macroions, there is no meaningful definition of a WS cell. Hence, it is difficult to define the volume fraction η reasonably. Provided that the WS cell can be considered as a sphere around a macroion, we can come up with two boundaries: The WS cell should not penetrate the Debye layer, thus $R \geq r_{\mathrm{ov}}^{(1)}/2 = \kappa^{-1} + \sigma/2$. In addition, the two WS cells should not overlap, hence, $R \leq r/2$. Note that the upper boundary depends on the macroion separation, whereas, according to theory, κ is not a function of r. However, our simulation data indicate that $\frac{d}{dr}\kappa_{\mathrm{eff}}$ is slightly different from zero. Taking into account both limits of R, the volume fraction $\eta = n_c(\frac{\sigma}{2R})^3$ should fullfill the inequality $(1 + \frac{2}{\kappa\sigma})^{-1} < \eta^{1/3} < \frac{\sigma}{r}$. With κ from Eq. (2), the lower boundary takes values from 1.6 $\times 10^{-2}$ ($n_s = 0$) to 9.3×10^{-2} ($n_s = 1280$). The overall volume

fraction of macroions in our simulation box is given by η' = $\frac{\pi\sigma^3}{3V} \approx 2.1 \times 10^{-3}$. Hence, in dilute systems, η' cannot be regarded as the relevant volume fraction for testing Alexander's charge-renormalization concept. Moreover, $\eta' \ll 1$ indicates that Eq. (9) should hold at least for small salt concentrations, provided that γ_0 can be neglected, i.e., $\kappa_{\mathrm{eff}} \approx \kappa$. Although both values, Z_{eff} and κ_{eff}, are not found to be in agreement with DH theory, their relation seems to be compatible with Eq. (9), as can be seen from Fig. 4. Thus, to a good approximation, the effective salt concentration matches the actual one, i.e., the Donnan effect is indeed negligible.

So far, we have addressed only the behavior of effective pair forces. In order to analyze the microionic degrees of freedom, we calculate the angular resolved negative charge-density distribution, $\rho_-(\alpha)$, which we define as follows: For a given macroion separation, we draw a sphere of radius $r/2$ around each macroion and project all counterions, which are located within this fictitious "WS cell", onto a plane that contains the macroions' centers (see the sketch in Fig. 5). $n_{\mathrm{ct}}(\alpha)$ is the number of counterions at angle α, which is taken relative to the connecting line to the other macroion, and $\rho_-(\alpha)$ is given by
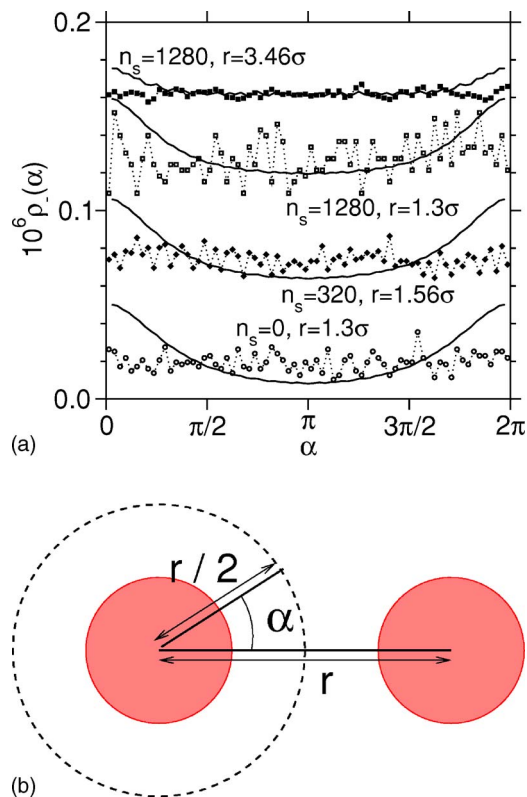

(a)

(b)

FIG. 5. (Color online) Angular resolved negative charge-density distribution around macroion [see sketch and the definition, Eq. (11)], for the indicated salt concentrations and macroion separations. Data sets are shifted by 0, 0.05, 0.1, and 0.15 (from below). The solid lines are calculated from the superposition of one-particle charge-density distributions from DH theory (for details, see the text).

$$\rho_-(\alpha) = 10^{-6} n_{ct}(\alpha) \left(\frac{\sigma_{mm}}{r}\right)^3. \tag{11}$$

Note that $\rho_-(\alpha)$ is normalized via the volume of the WS sphere, $\pi r^3/6$.

Figure 5 shows $\rho_-(\alpha)$ for various combinations of κr. Four different cases are considered: For $n_s = 0$, we choose r such that $\kappa_{eff} r \ll \kappa r_{ov}^{(3)}$. For $n_s = 320$, we consider the case $\kappa r_{ov}^{(3)} < \kappa_{eff} r < \kappa r_{ov}^{(2)}$. For $n_s = 1280$, we take $\kappa r_{ov}^{(3)} < \kappa_{eff} r < \kappa r_{ov}^{(2)}$ and $\kappa_{eff} r \gg \kappa r_{ov}^{(1)}$, respectively.

For an isolated pair of macroions, the electric field around a macroion only exhibits a spherical symmetry in the limit $\kappa r \to \infty$. Therefore, one might expect that $\rho_-(\alpha)$ is not independent of α, and thus it should reveal anisotropies. However, within the statistics of our data, we find flat distributions within the "WS cell". This holds even for the smallest value of κr, where the Debye layer around a given macroion is strongly perturbed by the other macroion. The occurrence of isotropic distributions $\rho_-(\alpha)$ might be due to nonlinearities, which are of course not accounted for in the DH limit. In order to rationalize this hypothesis, we checked whether $\rho_-(\alpha)$ can be "reconstructed" by a naive superposition of counterion charge distributions around a single macroion. To this end, we considered first such single-particle distributions as obtained from DH theory using the screening parameter κ as given by Eq. (2) and the bare charge Z for the charge of the macroion [note that the charge distribution is just proportional to the potential given by Eq. (6) in the linearized DH limit]. Then, we projected the superposition of the latter distributions onto a cubic lattice with 10^8 grid points. From this, we finally calculated $\rho_-(\alpha)$. The results are included in Fig. 5 as solid lines. We clearly see that the so calculated $\rho_-(\alpha)$ are anisotropic, and this indicates that the flat distributions obtained from the MD simulations might be due to the occurrence of nonlinearities.

The behavior of $\rho_-(\alpha)$ might also explain why the effective charge Z_{eff} is higher than the bare charge Z, in contrast to the prediction from the charge-renormalization concept. We can infer from the angular distributions $\rho_-(\alpha)$ that there are fewer counterions between the macroions than expected from a naive superposition principle. This effect might be of entropic origin, indicating that the entropy gain related to isotropic distributions dominates over energetic contributions. However, energetically unfavored microion distributions might yield an additional repulsion between the macroions, and this might explain the finding that Z_{eff} is larger than the bare charge.

We have already mentioned that the introduction of a "WS cell" is not appropriate for a system of two isolated macroions and thus cell models that lead to charge renormalization cannot be applied. There is also another reason why the concept of charge renormalization is not appropriate in the present case. If we define the boundary of the (spherical) "WS cell" by the sphere of radius $R = r/2$ around a macroion, this cell is not a neutral object, i.e., the total charge inside the cell is nonzero. This is in contrast to the assumptions of Alexander's cell model, which is not applicable for small macroion separations.
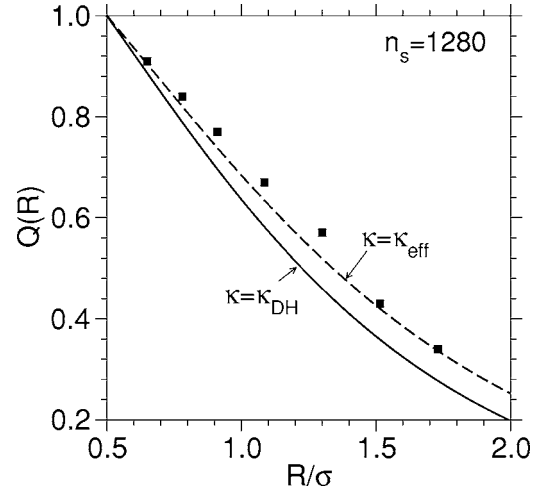

FIG. 6. Deviation from charge neutrality within "WS cell", measured via $Q(R)$, as defined in Eq. (13). Data are plotted for $n_s = 1280$. Results are compared to Eq. (16), using κ from Eq. (2) (solid line) and κ_{eff} (dashed line).

However, it is instructive to study the total charge of the "WS cell" for our system. Charge neutrality requires

$$Z \left(\frac{\sigma_m}{2R}\right)^3 + \int_0^{2\pi} d\alpha \rho_+(\alpha) = \int_0^{2\pi} d\alpha \rho_-(\alpha), \tag{12}$$

where $\rho_+(\alpha)$ has an analogous definition as $\rho_-(\alpha)$, but now the number of counterions at angle α is replaced by the corresponding number of coions. It follows from Eq. (12) that

$$Q(R) \equiv 1 + \frac{1}{Z} \left(\frac{2R}{\sigma_m}\right)^3 \int_0^{2\pi} d\alpha [\rho_+(\alpha) - \rho_-(\alpha)] \tag{13}$$

should vanish if the overall charge within the "WS cell" is zero. In Fig. 6, we show $Q(R)$ for a fixed salt concentration of $n_s = 1280$. It is compared to an estimate that follows from DH theory: Suppose the counterion density around a macroion is given by an expression of the DH form,

$$\rho(r) = \frac{\gamma \exp\left[-\kappa\left(r - \frac{\sigma}{2}\right)\right]}{\left(1 + \frac{\kappa\sigma}{2}\right) r \lambda_B^2}, \tag{14}$$

where γ is a dimensionless normalization constant. Since $Q(R) = 1 - \frac{1}{Z} \int_{V(r)} d^3 r \rho(\mathbf{r})$, the total charge reads

$$Q(R) = 1 - \frac{4\pi}{Z} \int_{\sigma/2}^R dr r^2 \rho(r) = 1 - \frac{4\pi\gamma}{Z \lambda_B^2 \left(1 + \frac{\kappa\sigma}{2}\right)} \left\{ \frac{\sigma}{2\kappa} + \frac{1}{\kappa^2} \right.$$

$$\left. - \left(\frac{R}{\kappa} + \frac{1}{\kappa^2}\right) \exp\left[-\kappa\sigma\left(\frac{R}{\sigma} - \frac{1}{2}\right)\right] \right\}. \tag{15}$$

The normalization constant introduced in Eq. (14) is determined by the boundary condition $Q(R \to \infty) \to 0$, thus $\gamma = \frac{Z \lambda_B^2 (1 + \kappa\sigma/2)}{4\pi(\sigma/2\kappa + 1/\kappa^2)}$. Hence, the charge inside the fictitious WS cell of radius R is given by the expression

$$Q(R) = \frac{1 + \kappa R}{1 + \frac{\kappa\sigma}{2}} \exp\left[-\kappa\sigma\left(\frac{R}{\sigma} - \frac{1}{2}\right)\right]. \quad (16)$$

Note that the second boundary condition, $Q(R=\frac{\sigma}{2})=1$, is intrinsically fulfilled. If we identify the inverse screening length as κ from Eq. (2), Eq. (16) slightly underestimates $Q(R)$. Replacing κ by the effective inverse screening length leads to an almost perfect agreement with the results of our simulations.

B. Three macroions

In this section, we consider systems with three macroions in two different geometries by placing them along a line or at the corners of an equilateral triangle.

In general, the interaction energy for three particles can be written as

$$V(r) = V_{12}(r_{12}) + V_{13}(r_{13}) + V_{23}(r_{23}) + V_{123}(r_{123}), \quad (17)$$

where $V_{ij}(r_{ij})$ is the pair potential between particle i and j. The last term on the right-hand side represents the three-body interactions.

We measure the force on the outermost particle (particle "1") and define the relative deviation of the electric field with respect to the expectation for pairwise additivity by

$$\Delta \equiv \frac{\frac{\partial}{\partial r}[V(r) - V(r_{12}) - V(r_{13})]}{\frac{\partial}{\partial r}V(r)} = \frac{E^{(3)} - E^{(2)}}{E^{(3)}}. \quad (18)$$

Here, $E^{(2)}$ is the superposition of the two-body interactions calculated in the previous subsection, whereas $E^{(3)} = -\frac{1}{Z}\frac{\partial}{\partial r}V(r)$ follows from the force acting on the outermost particle in the three-macroion configuration.

For the coaxial geometry, the pair contribution is given by $E^{(2)} = -\frac{1}{Z}\frac{\partial}{\partial r}\Sigma_{i>1}V(r_{1i})$. In the configuration of an equilateral triangle with side length R, one has to take into account that the forces do not act along the same direction. If we denote the positions of the macroions by $\vec{R}_i$ ($i=1,2,3$), the effective force $F(R)$ is given by the total force $\vec{F}_1$ on particle 1 projected onto the difference vector $\vec{d}=\vec{R}_1 - \frac{1}{3}(\vec{R}_1 + \vec{R}_2 + \vec{R}_3)$,

$$F(R) = \vec{F}_1 \cdot \frac{\vec{d}}{|\vec{d}|}. \quad (19)$$

Thus, the two-body contribution in the equilateral triangle is $E^{(2)} = -\frac{1}{Z}\frac{\partial}{\partial r}\Sigma_{i>1}V(r_{1i})\cos(\pi/6)$.

Results for the coaxial geometry are displayed in Fig. 7, where the deviation Δ from pairwise additivity is plotted as a function of the parameter $f_{ov}^{ca} \equiv \frac{\kappa\sigma}{2}\left[\frac{(r_{12}+r_{23})}{\sigma} - 1\right]$. The quantity f_{ov}^{ca} describes the overlap between the Debye layers around the three macroions. For $f_{ov}^{ca} < 1$, the three Debye layers exhibit an overlap.

One can infer from Fig. 7 that the three-body interaction between the macroions yields attractive corrections to pair-
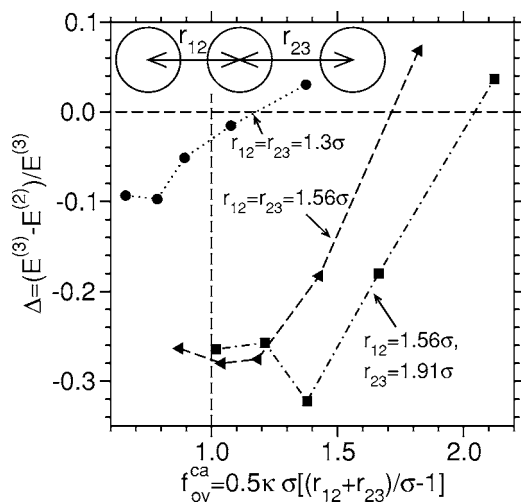

FIG. 7. Relative deviation Δ of electric field around the outermost macroion in the coaxial geometry as compared to expectation for pairwise additivity for different distances r_{12} and r_{23} between the particles.

wise additivity. At small salt concentration, i.e., if f_{ov}^{ca} is significantly smaller than one for a given distance between the macroions, three-body corrections are most pronounced and they are weakly dependent on f_{ov}^{ca}. But if f_{ov}^{ca} reaches values that are of the order of 1, the parameter Δ increases rapidly and seems to vanish at high values of f_{ov}^{ca}. Thus, three-body contributions are of importance if there is an overlap between the three Debye layers. This shows that the range of three-body contributions is of the order of the Debye length and thus the concept of screening is also very useful for the discussion of many-body effects.

It is interesting that the three-body terms are much smaller in the coaxial geometry if the distance between neighboring macroions is close to contact. This corresponds to the data for $r_{12}=r_{23}=1.3\sigma$ in Fig. 7. In this case, the pair interaction is probably the most important contribution because the three-body force on the outermost particle is effectively screened out by the particle in the middle.

In the case of an equilateral triangle, the condition for three overlapping Debye layers reads $f_{ov}^{tr} \equiv \kappa\sigma\left(\frac{r}{\sqrt{3}\sigma} - \frac{1}{2}\right) < 1$. Using the same values of κ and r for both geometries leads to $f_{ov}^{tr} < f_{ov}^{ca}$, thus, in the triangular configuration, the Debye layers exhibit a stronger overlap.

In Fig. 8, three different geometries for the macroion triple are compared: (i) an equilateral triangle with side length $r=1.3\sigma$, (ii) an equilateral triangle with side length $r=1.82\sigma$, and (iii) the coaxial geometry with $r=r_{12}=r_{23}=1.3\sigma$.

The strongest triplet interactions are revealed for case 1. Different from the coaxial geometry, the magnitude of the parameter Δ increases with decreasing distance r between the particles in the triangle. This can be easily understood since the interaction between the three macroions in the triangular geometry is not effectively screened by one of them but only by the microions in the Debye layers. For case 1, the magnitude of the parameter Δ also seems to increase with increasing f_{ov}^{tr}. As of yet, we do not have an explanation for this behavior.
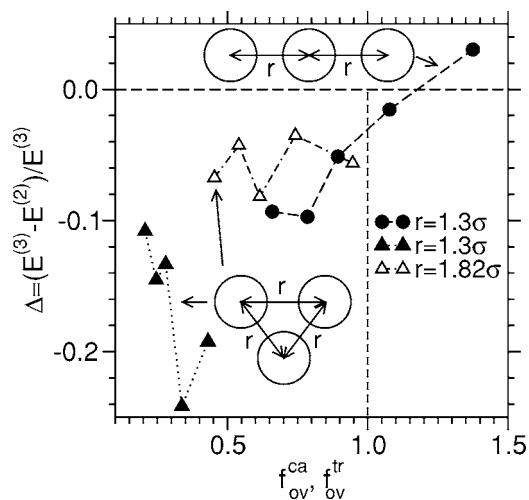
FIG. 8. Relative deviation of electric field around the macroion as compared to expectation for pairwise additivity vs overlap factor f_{ov} (see text). Triangular symbols represent triangular setup, circles represent coaxial geometry.
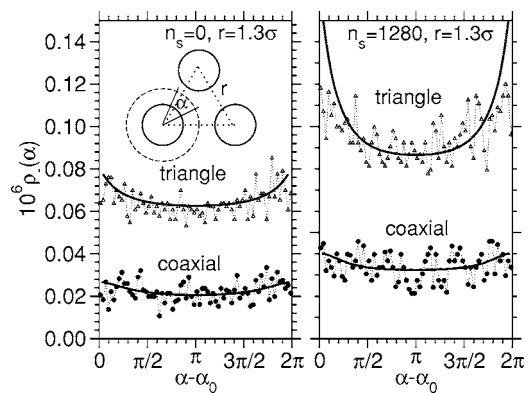

FIG. 9. Negative charge-density distribution for the three-macroion case, comparing the coaxial geometry to the triangular configuration. The latter is shifted by -0.05. The macroion separation is fixed to $r=1.3\sigma$. Salt concentration is $n_s=0$ (left) and $n_s =1280$ (right), respectively. Solid lines have same meaning as in Fig. 5.

V. CONCLUDING REMARKS

We performed classical MD simulations in order to investigate effective interactions between isolated pairs and triples of charged macroions in the framework of the primitive model.

On the pair level, these interactions are surprisingly well described by the DH limit of the PB equation. In particular, there is no evidence for charge renormalization as predicted by cell models. These models would predict an effective charge that is considerably smaller than the bare charge of the macroion [6,7,15]. This finding is not due to finite-size effects in the simulation that might emerge if the Debye length exceeds the size of the simulation box. It rather follows from the fact that the cell model must not be applied to systems of isolated macroions. This means that the concept of charge renormalization might be relevant for bulk systems, but, in the case of systems of isolated macroions, simulations should be compared to direct solutions of the nonlinear PB equation.

In this work, we have studied systems with salt concentrations of the order of 10^{-3} to 10^{-4} mol/l, and we have considered configurations for which the Debye layers of the different macroions exhibit a strong overlap. An interesting result of our simulations is the occurrence of repulsive corrections to DH theory: For the macroion pair, we find effective macroion charges that are slightly higher than their bare charge. Similar results have been reported in previous work, e.g., in an *ab initio* density-functional-theory approach [14], where the ratio between effective and bare charge was found to be between 1.06 and 1.38, depending on salt concentration and the value of the bare charge. A "repulsive correction to DH theory" is also indicated by the isotropic charge distribution around the macroion in the case of the macroion pair. Such an isotropic distribution is not expected from a naive superposition of one-particle density distributions as obtained from DH theory. Hence, there seem to be fewer counterions between the macroions than expected from DH theory, which can be related to an increase of the effective

Comparing cases (ii) and (iii), we see that deviations from pairwise additivity are similar in both cases, and the overlap parameters f_{ov}^{tr} and f_{ov}^{ca} have comparable values. A similar feature has been found in a numerical solution of the nonlinear PB equation by Russ *et al.* [16]. These authors report that the three-body potential is independent of geometry if the sum over the distances between neighboring particles is constant.

We would like to point out that there is always a trivial contribution to the many-body potential, which stems from an increased microion concentration associated with the addition of macroions. Thus, for a fixed volume, the effective screening length of the system is decreased. A comparison between the measured three-body term, $E^{(3)}$, and the two-body contribution, $E^{(2)}$, taken from the pure two-macroion case should therefore in general yield a nonpairwise additivity. From that point of view, DH theory already predicts a correction to pairwise additivity.

Similar to the previous subsection, we calculate the angular resolved charge-density distribution around the outermost macroion [see Eq. (11)]. In order to account for the differences between coaxial and triangular geometry, we introduce an angle α_0, such that the system is symmetric around $\alpha =\alpha_0$. Thus, we have to choose $\alpha_0=0$ for the coaxial geometry and $\alpha_0=\pi/6$ for the equilateral triangle.

As Fig. 9 shows, the charge distribution for the three-macroion case is not isotropic. From Fig. 9 we can infer that the onset of anisotropy is correlated with nonpairwise additivity. Consistent with the behavior of the parameter Δ in Fig. 8, the choice of the same value of r leads to a stronger anisotropy for the triangle as compared to the coaxial geometry. As done in the previous section, we compare our charge distribution to the one that follows from a naive superposition of the DH distributions. Surprisingly, for the three-macroion configurations, this superposition seems to work very well.

charge. The microscopic origin of this effect is not clear, but it might be of entropic origin.

In agreement with previous analytical [10], numerical [12,16,18], and experimental studies [8,9] of systems with three isolated macroions, we find that corrections to nonpairwise additivity (and thus the three-body terms in the effective potential) are attractive. The strength of these attractive contributions is strongly correlated with the overlap of all three Debye layers. This shows that the concept of a screening length is also very useful to quantify the effect of three-body interactions. Different from the case of two macroions, the charge distribution in the three-macroion case is anisotropic. In this case, the simple superposition of three one-particle density distributions from DH theory yields a rather good description of the charge distribution in the three-macroion case. This finding seems to agree with a recent numerical solution of the PB equation for three isolated macroions [16].

In further simulation studies, we will investigate interactions between more than three particles to understand the crossover to bulk effective interactions. In the latter case, the concept of charge renormalization seems to work very well. Our present simulations suggest that many-body interactions in bulk systems yield renormalized charges that can be much smaller than the bare charges of charged colloidal particles. A profound understanding of these issues might also provide new insight into electrophoresis experiments [19,20].

[1] L. Belloni, J. Phys.: Condens. Matter **12**, R549 (2000).

[2] A. A. Louis, J. Phys.: Condens. Matter **14**, 9187 (2002).

[3] W. B. Russel, D. A. Saville, and W. R. Schowalter, *Colloidal Dispersions* (Cambridge University Press, Cambridge, 1989).

[4] B. Derjaguin and L. Landau, Acta Physicochim. URSS **14**, 633 (1941); E. J. W. Verwey and J. T. G. Overbeck, *Theory of the Stability of Lyotropic Colloids* (Elsevier, Amsterdam, 1948).

[5] P. Debye and E. Hückel, Phys. Z. **24**, 185 (1923).

[6] S. Alexander, P. M. Chaikin, P. Grant, G. J. Morales, P. Pincus, and D. Hone, J. Chem. Phys. **80**, 5776 (1984).

[7] E. Trizac, L. Bocquet, M. Aubouy, and H. H. von Grünberg, Langmuir **19**, 4027 (2003).

[8] M. Brunner, J. Dobnikar, H. H. von Grünberg, and C. Bechinger, Phys. Rev. Lett. **92**, 078301 (2004).

[9] J. Dobnikar, M. Brunner, H. H. von Grünberg, and C. Bechinger, Phys. Rev. E **69**, 031402 (2004).

[10] A. R. Denton, Phys. Rev. E **70**, 031404 (2004).

[11] E. Allahyarov, H. Löwen, and S. Trigger, Phys. Rev. E **57**, 5818 (1998).

[12] H. Löwen and E. Allahyarov, J. Phys.: Condens. Matter **10**, 4147 (1998).

[13] E. Allahyarov and H. Löwen, Phys. Rev. E **63**, 041403 (2001).

[14] R. Tehver, F. Ancilotto, F. Toigo, J. Koplik, and J. R. Banavar, Phys. Rev. E **59**, R1335 (1999).

[15] L. Shapran, M. Medebach, P. Wette, T. Palberg, H. J. Schöpe, J. Horbach, T. Kreer, and A. Chatterji, Colloids Surf., A **270–271**, 220 (2005).

[16] C. Russ, H. H. von Grünberg, M. Dijkstra, and R. van Roij, Phys. Rev. E **66**, 011402 (2002).

[17] M. P. Allen and D. J. Tildesley, *Computer Simulation of Liquids* (Clarendon, Oxford, 1987).

[18] J. Z. Wu, D. Bratko, H. W. Blanch, and J. M. Prausnitz, J. Chem. Phys. **113**, 3360 (2000).

[19] N. Garbow, M. Evers, T. Palberg, and T. Okubo, J. Phys.: Condens. Matter **16**, 3835 (2004).

[20] M. Medebach and T. Palberg, J. Phys.: Condens. Matter **16**, 5653 (2004).